Inclusive transverse response of nuclear matter

Adelchi Fabrocini
Department of Physics, University of Pisa and Istituto Nazionale di Fisica Nucleare, Sezione di Pisa, I-56100 Pisa, Italy
(Received 11 September 1996)

The electromagnetic inclusive transverse response of nuclear matter at saturation density is studied within the correlated basis function perturbation theory for momentum transfers q from 300 to 550 MeV/c. The correlation operator includes a Jastrow component, accounting for the short range repulsion, as well as longer range spin, tensor, and isospin ones. Up to correlated one-particle–one-hole intermediate states are considered. The spreading due to the decay of particle (hole) states into two-particle–one-hole (two-hole–one-particle) states is considered via a realistic optical potential model. The Schiavilla-Pandharipande-Riska model for the two-body electromagnetic currents, constructed so as to satisfy the continuity equation with realistic v_{14} potentials, is adopted. Currents due to intermediate Δ-isobar excitations are also included. The global contribution of the two-body currents turns out to be positive and provides an enhancement of the one-body transverse response ranging from $\sim$20% for the lower momenta to $\sim$10% for the higher ones. This finding is in agreement with the Green's function Monte Carlo studies of the transverse Euclidean response in $A=3,4$ nuclei and contradicts previous results obtained within the Fermi gas and shell models. The tensor-isospin component of the correlation is found to be the leading factor responsible for such a behavior. The nuclear matter response is compared to recent experimental data on ^{40}Ca and ^{56}Fe. [S0556-2813(97)04801-2]

PACS number(s): 21.65.+f, 21.30.Fe, 24.10.Cn, 25.70.−z

I. INTRODUCTION

The cross section for inclusive electron scattering at intermediate three-momentum transfers ($q \leqslant 600$ MeV/c) has been the object of many theoretical and experimental investigations. In the one-photon-exchange approximation the differential cross section is given by

$$\frac{d^2\sigma}{d\Omega d\omega} = \sigma_M \left\{ \frac{q_\mu^4}{q^4} R_L(q,\omega) + \left[\tan^2\left(\frac{\theta}{2}\right) - \frac{q_\mu^2}{2q^2} \right] R_T(q,\omega) \right\}, \tag{1}$$

where σ_M is the Mott cross section, $q_\mu^2 = \omega^2 - q^2$ is the squared four-momentum transfer, θ is the scattering angle, and $R_{L(T)}(q,\omega)$ is the longitudinal (transverse) separated response.

The total cross section is indeed well described by a simple Fermi gas (FG) model [1], but the agreement disappears when the longitudinal-transverse (L/T) separation [2–9] is carried out for medium-heavy nuclei. R_L is largely overestimated by the FG model. However, the quenching of the longitudinal response is now well understood in terms of short range dynamical correlations, induced by the strong nucleon-nucleon (NN) interaction, and of nucleon degrees of freedom alone.

In Ref. [10] a realistic model of correlated nuclear matter (NM) was used to study $R_L(q,\omega)$ at the NM empirical saturation density, in the framework of the correlated basis function (CBF) theory. The density-dependent nuclear matter CBF results have then been used in Ref. [9] to estimate the longitudinal response in ^{12}C, ^{40}Ca, and ^{56}Fe in the local density approximation (LDA). The overall agreement with the experimental data was shown to be satisfactory.

The present understanding of $R_T(q,\omega)$ is more uncertain. Recent experimental L/T separations in ^{40}Ca [6,9] have provided a transverse response lower than previous estimates [4] at the quasielastic (QE) peak. On the other side, theoretical realistic calculations (feasible in the longitudinal case) have been so far prevented by the complicated structure of the transition operator, containing one- and two-body currents. In light nuclei ($A=3,4$) only the Euclidean transverse response, with the full current operator, has been computed [11] using the exact Green's function Monte Carlo (GFMC) technique and the realistic Argonne v_{14} NN interaction [12]. The GFMC technique cannot be presently adopted in heavier nuclei, and so studies of $R_T(q,\omega)$ in these systems either have considered only the easier to address one-body piece [13,14] or have treated the two-body meson exchange currents (MEC's) within independent particle models (IPM's) [15–17]. The MEC's were found to substantially increase the one-body response in Ref. [11], whereas the IPM calculations of Ref. [17] point to a slight reduction. It is worth noticing that the aforementioned latest heavy-nuclei-separated $R_T(q,\omega)$ show a good agreement with theoretical responses containing only one-body currents [9], downplaying the role of the MEC's and in contrast with both the light nuclei case and the old ^{40}Ca data.

Aim of this work is to use CBF theory to compute the symmetric nuclear matter transverse response in order to ascertain how it is affected by the NN correlations. Particular attention will be devoted to their influence on the MEC contribution. The results presented in this paper have been obtained within the exchange current operator model developed by Schiavilla, Pandharipande, and Riska (SPR) in Ref. [18]. The SPR model satisfies the continuity equation linking the current to the NN interaction and contains intermediate Δ-isobar excitations. For the sake of comparison, also the standard one-pion-exchange currents have been used.

In nuclear matter, CBF calculations are based upon a set of *correlated* wave functions

$$|n\rangle = \mathcal{S}\left[\prod_{i<j} f(i,j)\right]|n\rangle_{\rm FG}, \tag{2}$$

obtained by applying a symmetrized product of two-body correlation operators, $f(i,j)$, to the FG states $|n\rangle_{\rm FG}$. An effective structure for $f(i,j)$ is

$$f(i,j) = \sum_{q=1,6} f^{(q)}(r_{ij}) O_{ij}^{(q)},$$

$$O_{ij}^{(q=1,6)} = (1, \boldsymbol{\sigma}_i \cdot \boldsymbol{\sigma}_j, S_{ij}) \otimes (1, \boldsymbol{\tau}_i \cdot \boldsymbol{\tau}_j), \tag{3}$$

S_{ij} being the tensor operator; this operatorial dependence resembles the structure of the NN interaction. Additional spin-orbit correlations are often considered in realistic NM ground state (g.s.) studies; however, they will not be taken into account in this work. $f(i,j)$ depends upon a set of variational parameters, which are fixed by minimizing the expectation value of a realistic, nonrelativistic Hamiltonian on the correlated ground state. The g.s. energy is calculated via the Fermi hypernetted chain (FHNC) cluster summation technique [19] and the operatorial contributions ($q>1$) are implemented by the single operator chain (SOC) (and successive improvements) approximation [20,21]. We have used the correlation corresponding to the Argonne v_{14}+Urbana VII three-nucleon interaction model of Ref. [21]. A model with a weaker tensor force (the Urbana v_{14}+TNI interaction [22]) was adopted for the CBF studies of $R_L(q,\omega)$ in Ref. [10] and of the L/T spin responses in Ref. [23].

The correlation given in Eq. (3) contains a $q=1$ scalar (or Jastrow) component $f^J(r)$, almost vanishing at short distances, so that configurations where two nucleons are close enough are essentially suppressed in the wave function because of the short range NN repulsion. $f^J(r)$ heals to unity at large distances. The most important among the remaining components are, by far, the $q=5$, spin-isospin, $f^{\sigma\tau}(r)$ and the $q=6$, tensor-isospin, $f^{t\tau}(r)$ ones, which are related to the one-pion-exchange (OPE) long range part of the potential [21].

The response is computed by considering up to correlated one-particle-one hole ($1p1h$) intermediate states. Admixtures of correlated particle (hole) states with $2p1h(2h1p)$ ones are accounted for by the optical potential model of Ref. [24]. This model has been proven to be fairly accurate in the momentum region scanned here, at least for the longitudinal response [10]. No correlated $2p2h$ intermediate states have been considered, since they contribute mainly at larger energies than those of the QE peak [17], which is the focus of this work. A peak due the excitation of Δ resonances is also present in the transverse response at high energies. The Δ peak is, however, well distinct from this quasielastic one and it has not been studied in the paper. It would have required the introduction of Δ degrees of freedom in the nuclear wave function.

The plan of the paper is as follows. The CBF approach to the transverse response is sketched and the current operators are briefly described in Sec. II. Section III is devoted to the discussion of the matrix elements of the current. The numerical results are presented and discussed in Sec. IV, together with a comparison with some of the available experimental data. Finally, some conclusions are drawn.

II. CURRENT OPERATOR AND THE CBF THEORY OF THE TRANSVERSE RESPONSE

The transverse response $R_T(q,\omega)$ is given by

$$R_T(q,\omega) = \frac{1}{A}\sum_n |\langle 0|\mathbf{j}(\mathbf{q})|n\rangle|^2 \delta(\omega-\omega_n), \tag{4}$$

where the sum goes over the intermediate excited states $|n\rangle$, having excitation energy ω_n, and $\mathbf{j}(\mathbf{q})$ is the electromagnetic current operator. $\mathbf{j}(\mathbf{q})$ has contributions from one-body $\mathbf{j}^{(1)}(\mathbf{q})$ and two-body $\mathbf{j}^{(2)}(\mathbf{q})$ exchange currents. In the impulse approximation (IA) only $\mathbf{j}^{(1)}(\mathbf{q})$ is retained.

$\mathbf{j}^{(1)}(\mathbf{q})$ is the sum of the convection $\mathbf{j}_C^{(1)}(\mathbf{q})$ and magnetization $\mathbf{j}_M^{(1)}(\mathbf{q})$ terms. However, it is known that the convection current contributes significantly to the non-energy-weighted sum of the response at very low q values, where it becomes dominant [25]. At momentum transfers $\geqslant 150$ MeV/c it provides only a few percent of the total sum, with a correction going as $1/q^2$. For this reason, $\mathbf{j}_C^{(1)}(\mathbf{q})$ has not been considered here and we have approximated

$$\mathbf{j}^{(1)}(\mathbf{q}) \sim \mathbf{j}_M^{(1)}(\mathbf{q}) = \imath G(q,\omega)\frac{\mu_0}{e}\sum_{i=1,A} e^{\imath \mathbf{q}\cdot\mathbf{r}_i}\left[\mu_p \frac{1+\tau_{i,z}}{2} + \mu_n \frac{1-\tau_{i,z}}{2}\right]\boldsymbol{\sigma}_i \times \mathbf{q}, \tag{5}$$

where μ_0 is the nuclear magneton and $\mu_{p,n}$ are the nucleon magnetic moments. The dipole parametrization has been used for the nucleon form factor $G(q,\omega)$, with a scale parameter of 839 MeV. Studying the dependence of the response to the different available parametrizations of the electromagnetic nucleon form factors is beyond the scope of the present paper.

$\mathbf{j}_M^{(1)}(\mathbf{q})$ can be written in terms of the isoscalar and isovector transverse spin fluctuation operators $\rho_{T,\sigma}^{\tau=0,1}(\mathbf{q})$,

$$\rho_{T,\sigma}^{0(1)}(\mathbf{q}) = \frac{1}{\sqrt{2}}\sum_{i=1,A} e^{\imath \mathbf{q}\cdot\mathbf{r}_i}(\boldsymbol{\sigma}_i \times \mathbf{q})(\tau_{i,z}), \tag{6}$$

and, correspondingly, the IA electromagnetic response is related to the spin structure functions $S_{T,\sigma}^{0,1}(\mathbf{q},\omega)$ by

$$R_T^{\rm IA}(q,\omega) = \left(\frac{\mu_0}{e\sqrt{2}}\right)^2 |G(q,\omega)|^2 [\mu_+^2 S_{T,\sigma}^0(\mathbf{q},\omega) + \mu_-^2 S_{T,\sigma}^1(\mathbf{q},\omega)], \tag{7}$$

where $\mu_\pm = \mu_p \pm \mu_n$. $S_{T,\sigma}^{0,1}(\mathbf{q},\omega)$ have been computed in Ref. [23] in FHNC SOC. So the details of the CBF calculation of the IA transverse response will not be discussed here.

Most of the studies on exchange currents are based on simple meson exchange mechanims, in a nonrelativistic description of the nucleon-meson-Δ systems [26]. In this case MEC's associated with one-pion exchange are given by the sum of three terms, obtained by the corresponding Feynman diagrams: the contact or seagull term $\mathbf{j}_{\rm cont}^{(2)}(\mathbf{q})$, the pionic or

pion in flight term $\mathbf{j}_\pi^{(2)}(\mathbf{q})$, and the Δ term $\mathbf{j}_\Delta^{(2)}(\mathbf{q})$ associated with the excitation of intermediate Δ resonances. Analogous contributions arise from one-rho exchange. Their expressions can be found in several papers and, among them, in Ref. [18]. These currents are consistent with *NN* potentials based only on one-boson exchange (OBE), and so the continuity equation

$$\nabla\cdot\mathbf{j}(\mathbf{x};\mathbf{r}_1,\mathbf{r}_2)+\imath[v(\mathbf{r}_1,\mathbf{r}_2),\rho(\mathbf{x})]=0 \tag{8}$$

with realistic potentials is not satisfied.

In Ref. [18], the authors have derived exchange currents satisfying the continuity equation with Argonne and Urbana v_{14} potentials. The current was separated in the sum of a model-independent (MI) component, constructed from the *NN* interaction, and a model-dependent (MD) one, purely transverse and given by the previously introduced π and ρ MEC's with intermediate Δ excitations.

The most important MI currents are those associated with the isospin-dependent parts of the *NN* interaction. The corresponding current operators $\mathbf{j}_{PS}^{(2)}(\mathbf{q})$, $\mathbf{j}_V^{(2)}(\mathbf{q})$, and $\mathbf{j}_{VS}^{(2)}(\mathbf{q})$ are given in Ref. [18]. They are expressed in terms of the Fourier tranforms of the $v^{\tau}(r)$,$v^{\sigma\tau}(r)$, and $v^{t\tau}(r)$ parts of the potential [18] and reduce to the standard π and ρ MEC's if the OBE interaction is used. Argonne v_{14} has been used to generate the MI currents: they are close to those due to π and ρ exchanges, even if the interaction does not strictly have the OBE form.

The MD part of the current was associated with π and ρ MEC's with intermediate Δ excitations and to $\rho\pi\gamma$ and $\omega\pi\gamma$ currents, all of them treated within the OBE model. The last two currents will not be considered here. Later, Δ's were explicitly included in the wave function [27], instead of introducing effective two-body operators acting on nucleon coordinates, as in standard first order perturbation theory. These components were generated by transition correlation operators $U_{ij}^{TR}=U_{ij}^{N\Delta}+U_{ij}^{\Delta N}+U_{ij}^{\Delta\Delta}$ acting on realistic nuclear wave functions and obtained via the Argonne v_{28} [12] potential, which contains Δ degrees of freedom. Hence, $N\rightarrow\Delta$ and $\Delta\rightarrow\Delta$ transition operators were introduced in the one-body current. The Δ contribution to low-energy electroweak transitions was found to be smaller than that of perturbative theories as a consequence of this more realistic approach. It was also noticed that a first order perturbative treatment, consistent with that of Ref. [27], is obtained by using

$$u_{PT}^{\sigma(t)\pi\mathrm{II}}(r_{ij})=\frac{v^{\sigma(t)\pi\mathrm{II}}(r_{ij})}{m_N-m_\Delta}, \tag{9}$$

for the $N\rightarrow\Delta$ spin- and tensor-isospin transition correlations, where $v^{\sigma(t)\pi\mathrm{II}}$ are the corresponding transition components of the Argone v_{28} potential.

The intermediate Δ current generated in this way will be used. Its configuration space expression [28] is

$$\begin{aligned}\mathbf{j}_{\mathrm{MD}}^{(2)}(\mathbf{q})=\imath\tfrac{2}{9}G_\Delta(q,\omega)\mu_{\gamma N\Delta}\sum_{i<j}[&e^{\imath\mathbf{q}\cdot\mathbf{r}_i}(4\boldsymbol{\tau}_{j,z}\{[u_{PT}^{\sigma\tau\mathrm{II}}(r)-u_{PT}^{t\tau\mathrm{II}}(r)]\boldsymbol{\sigma}_j\times\mathbf{q}+3u_{PT}^{t\tau\mathrm{II}}(r)\hat{\mathbf{r}}\times\mathbf{q}(\boldsymbol{\sigma}_j\cdot\hat{\mathbf{r}})\}\\&-(\boldsymbol{\tau}_i\times\boldsymbol{\tau}_j)_z\{[u_{PT}^{\sigma\pi\mathrm{II}}(r)-u_{PT}^{t\pi\mathrm{II}}(r)](\boldsymbol{\sigma}_i\times\boldsymbol{\sigma}_j)\times\mathbf{q}+3u_{PT}^{t\pi\mathrm{II}}(r)(\boldsymbol{\sigma}_i\times\hat{\mathbf{r}})\times\mathbf{q}(\boldsymbol{\sigma}_j\cdot\hat{\mathbf{r}})\})+i\rightleftharpoons j].\end{aligned} \tag{10}$$

$\mathbf{r}=\mathbf{r}_{ij}$ and $\mu_{\gamma N\Delta}=3\mu_0$ is the transition magnetic moment adopted in Ref. [27], whose value is $\sim$30% smaller than the static quark model prediction [29]. For the Δ form factor we take

$$G_\Delta(q,\omega)=\left(1+\frac{q_\mu^2}{\Lambda_1^2}\right)^{-2}\left(1+\frac{q_\mu^2}{\Lambda_2^2}\right)^{-1/2}, \tag{11}$$

where the cutoff masses are $\Lambda_1=1196$ MeV and $\Lambda_2=843$ MeV.

As a result of the separation of the current into one- and two-body pieces, the response is given by

$$R_T(q,\omega)=R_T^{\mathrm{IA}}(q,\omega)+R_T^{\mathrm{int}}(q,\omega)+R_T^{\mathrm{MEC}}(q,\omega), \tag{12}$$

where $R_T^{\mathrm{int}}(q,\omega)$ is the interference contribution between $\mathbf{j}^{(1)}(\mathbf{q})$ and $\mathbf{j}^{(2)}(\mathbf{q})$,

$$\begin{aligned}R_T^{\mathrm{int}}(q,\omega)=\frac{1}{A}\sum_n\ &[\langle 0|\mathbf{j}^{(1)}(\mathbf{q})|n\rangle\langle n|(\mathbf{j}^{(2)}(\mathbf{q}))^\dagger|0\rangle+\mathrm{c.c.}]\\&\times\delta(\omega-\omega_n),\end{aligned} \tag{13}$$

and

$$R_T^{\mathrm{MEC}}(q,\omega)=\frac{1}{A}\sum_n\ |\langle 0|\mathbf{j}^{(2)}(\mathbf{q})|n\rangle|^2\delta(\omega-\omega_n). \tag{14}$$

$R_T^{\mathrm{int}}(q,\omega)$ and the leading term in $R_T^{\mathrm{MEC}}(q,\omega)$ only have been computed.

Let us now shortly discuss the most important aspects of the CBF perturbative expansion. The goal of using a correlated basis, embodying directly into the states some of the relevant physical effects (as the short range repulsion), is to obtain a rapidly converging expansion. The obvious price to be paid lies in the greater difficulty in evaluating matrix elements, even at the zeroth order. However, nuclear matter studies demonstrated that CBF-based perturbation theory is actually fast converging, in the sense (i) that for many observables the zeroth order is already a good estimate and (ii) that the inclusion of the first CBF intermediate states is often sufficient to provide a quantitative agreement with the empirical values. This happens for ground state properties, as the energy [30] and the momentum distribution [31], as well as for the already mentioned longitudinal and spin responses and the nucleon spectral function [32]. The inclusive electron

scattering cross section at high momentum transfers has been computed in Ref. [33], using the CBF spectral function, and satisfactorily compared with that extrapolated from data on laboratory nuclei.

Hence, relying on these facts, we will compute $R_T(q,\omega)$ by inserting in the intermediate state summation of Eq. (4) only correlated $1p1h$ states:

$$|\mathbf{ph}\rangle = \mathcal{S}\left[\prod_{i<j} f(i,j)\right]|\mathbf{ph}\rangle_{\rm FG}. \tag{15}$$

This choice is also justified on the ground that we are interested mainly in the QE peak. The quantitative study of the large energy region would have required the insertion of higher excited states with both nucleonic (as $2p2h$) and explicit Δ isobar excitations (as Δ-h).

The $1p1h$ transverse response is then given by

$$R_T^{1p1h}(q,\omega) = \frac{1}{A}\sum_{ph} |\langle 0|\mathbf{j}(\mathbf{q})|\mathbf{ph}\rangle|^2 \delta(\omega - e_p + e_h), \tag{16}$$

where $e_{x=p,h} = \langle \mathbf{x}|H|\mathbf{x}\rangle - \langle 0|H|0\rangle$ is the CBF variational (or zeroth order) single-particle energy of the x state.

The $1p1h$ response has sharp energy boundaries, qualitatively like the Fermi gas, ruled by the real part of the CBF optical potential, $U_k = e_k - \hbar^2 k^2/2m_N$ [30]. The decay of $1p1h$ states into $2p2h$ ones has the main effect of introducing a large energy tail and redistributing the strength. In the perturbative expansion this is accounted for by self-energy insertions on top of the particle or hole line. The real part of the self-energy provides a perturbative correction δe_x to the variational single-particle energy and the imaginary part induces the spreading of the response to high ω values. The microscopically computed CBF self-energy was used in the longitudinal response calculation of Ref. [10]. In Ref. [24] these corrections were estimated by folding the $1p1h$ response with a width $W(\omega)$ given by the imaginary part $W_0(\omega)$ of the optical potential divided by the nucleon effective mass,

$$R_T(q,\omega) = \frac{1}{\pi}\int d\omega' R_T^{1p1h}(q,\omega') \frac{W(\omega)}{(\omega-\omega')^2 + W(\omega)^2}, \tag{17}$$

with $W_0(\omega) \sim 11\omega^2/(4900+\omega^2)$, in MeV. This procedure, numerically much less involved and equivalent to retain the on-energy shell part of the self-energy only, was checked to be reliable in the momentum region of interest [10] and, for this reason, has been adopted here.

III. CBF MATRIX ELEMENTS OF THE CURRENT

This section will focus on the main features of the MEC CBF matrix elements. As far as the MI currents is concerned, only the leading $\mathbf{j}^{(2)}_{PS}(\mathbf{q})$ will be discussed. However, the contributions of the less influent $\mathbf{j}^{(2)}_{V}(\mathbf{q})$ and $\mathbf{j}^{(2)}_{VS}(\mathbf{q})$ have been evaluated and will be presented in the next section.

The configuration space PS current is written as a sum of two terms $\mathbf{j}^{(2)}_{PS,C}(\mathbf{q})$ and $\mathbf{j}^{(2)}_{PS,\pi}(\mathbf{q})$. The first one coincides with $\mathbf{j}^{(2)}_{\rm cont}(\mathbf{q})$ for the one-pion-exchange potential, the latter with $\mathbf{j}^{(2)}_{\pi}(\mathbf{q})$. Their expressions are

$$\mathbf{j}^{(2)}_{PS,C}(\mathbf{q}) = C_{PS}\sum_{i<j} 3(\boldsymbol{\tau}_i \times \boldsymbol{\tau}_j)_z \{e^{\imath \mathbf{q}\cdot\mathbf{r}_i} g_{PS}(r)\boldsymbol{\sigma}_i(\boldsymbol{\sigma}_j\cdot\hat{\mathbf{r}}) + i \rightleftharpoons j\} \tag{18}$$

and

$$\mathbf{j}^{(2)}_{PS,\pi}(\mathbf{q}) = C_{PS}\sum_{i<j} 3(\tau_i\times\tau_j)_z e^{\imath\mathbf{q}\cdot\mathbf{R}}\Bigg\{ \frac{G_{PS,1}(\mathbf{r})}{r^2}[\boldsymbol{\sigma}_i(\boldsymbol{\sigma}_j\cdot\hat{\mathbf{r}}) + \boldsymbol{\sigma}_j(\boldsymbol{\sigma}_i\cdot\hat{\mathbf{r}}) + \hat{\mathbf{r}}(\boldsymbol{\sigma}_i\cdot\boldsymbol{\sigma}_j)] + \imath\frac{G_{PS,2}(\mathbf{r})}{r}\boldsymbol{\sigma}_i(\boldsymbol{\sigma}_j\cdot\mathbf{q}) - \imath\frac{G_{PS,3}(\mathbf{r})}{r}\boldsymbol{\sigma}_j(\boldsymbol{\sigma}_i\cdot\mathbf{q})$$
$$- \imath\frac{G_{PS,4}(\mathbf{r})}{r}\hat{\mathbf{r}}(\boldsymbol{\sigma}_i\cdot\hat{\mathbf{r}})(\boldsymbol{\sigma}_j\cdot\mathbf{q}) + \imath\frac{G_{PS,5}(\mathbf{r})}{r}\hat{\mathbf{r}}(\boldsymbol{\sigma}_j\cdot\hat{\mathbf{r}})(\boldsymbol{\sigma}_i\cdot\mathbf{q}) - G_{PS,6}(\mathbf{r})\hat{\mathbf{r}}(\boldsymbol{\sigma}_i\cdot\mathbf{q})(\boldsymbol{\sigma}_j\cdot\mathbf{q}) - \imath\frac{G_{PS,7}(\mathbf{r})}{r^2}\hat{\mathbf{r}}(\boldsymbol{\sigma}_i\cdot\hat{\mathbf{r}})(\boldsymbol{\sigma}_j\cdot\hat{\mathbf{r}})\Bigg\}. \tag{19}$$

The functions $g_{PS}(r)$ and $G_{PS,\alpha=1,7}(\mathbf{r})$ are defined in Ref. [18], $\mathbf{R} = (\mathbf{r}_i + \mathbf{r}_j)/2$, and $C_{PS} = G(q,\omega)$.

In CBF theory the nondiagonal matrix elements $\xi_{PS,C(\pi)}(\mathbf{q};\mathbf{p},\mathbf{h}) = \langle 0|\mathbf{j}^{(2)}_{PS,C(\pi)}(\mathbf{q})|\mathbf{p},\mathbf{h}\rangle$ are computed by cluster expansions in Mayer-like diagrams, built up by dynamical correlations $f^{(q)}f^{(p)} - \delta_{q1}\delta_{p1}$ and by exchange links. Infinite classes of cluster terms containing Jastrow correlations are summed by FHNC. Less massive summations, similar to SOC's, can be performed for the operatorial correlations [10,24].

In the case of simple Jastrow correlated wave functions ($f^{q>1} = 0$), $\xi^J_{PS,C}$ is given by

$$\xi^J_{PS,C}(\mathbf{q};\mathbf{p},\mathbf{h}) = \delta_{\mathbf{q}-\mathbf{p}+\mathbf{h}}\imath C_{PS}\frac{6\tau_z}{\sqrt{D(p)D(h)}}\rho_0 \times \int d\mathbf{r} g_{PS}(r) g_{cc}(r)\{e^{\imath\mathbf{p}\cdot\mathbf{r}}(\hat{\mathbf{r}} - \imath\boldsymbol{\sigma}\times\hat{\mathbf{r}}) + e^{\imath\mathbf{h}\cdot\mathbf{r}}(\hat{\mathbf{r}} + \imath\boldsymbol{\sigma}\times\hat{\mathbf{r}})\}, \tag{20}$$

where $\tau_z = \tau_{p,z} = \tau_{h,z}$, $\boldsymbol{\sigma} = \boldsymbol{\sigma}_p = \boldsymbol{\sigma}_h$, $D(x=p,h) = 1 - X_{cc}(x)$ (see Ref. [24] for the definition of X_{cc}), $g_{cc}(r)$ is the exchange FHNC partial radial distribution function [19], and ρ_0 is the nuclear matter density. At the lowest

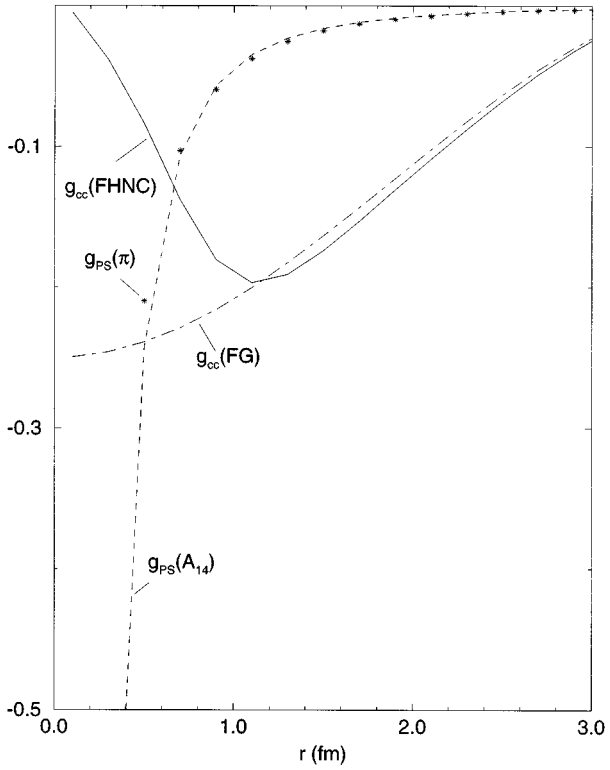

FIG. 1. $g_{\rm PS}$ functions for the Argonne v_{14}, $g_{PS}(A_{14})$, and the π exchange, $g_{PS}(\pi)$, potentials. g_{cc}(FHNC) and $g_{cc}(FG)$ are the correlated and uncorrelated exchange functions, respectively (see text).

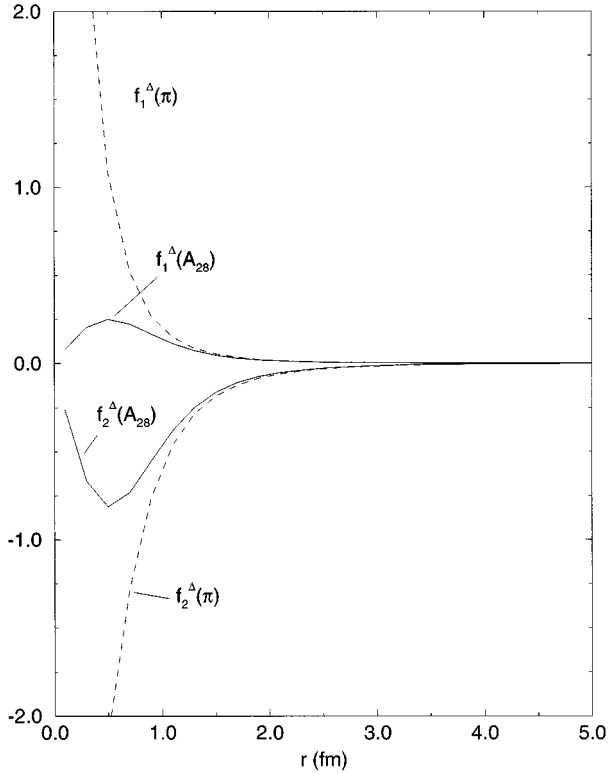

FIG. 2. $f^{\Delta}_{1,2}$ functions for the Argonne v_{28}, $f^{\Delta}_{1,2}(A_{28})$, and the π exchange, $f^{\Delta}_{1,2}(\pi)$, potentials.

order of the cluster expansion, $D(x)=1$ and $g_{CC}(r)=-[f^J(r)]^2 l(k_F r)/4$, where k_F is the Fermi momentum and $l(x)=3[\sin(x)-x\cos(x)]/x^3$ is the Slater exchange function. So Jastrow correlations suppress the short range part of the pionlike exchange interaction. This effect is visualized in Fig. 1, where the Argonne v_{14} g_{PS} and the FHNC g_{cc} functions are shown. Moreover, the figure compares g_{cc}(FHNC) with its uncorrelated Fermi gas counterpart, $g_{cc}(FG)=-l(k_F r)/4$, to stress their different short distance behaviors. Finally, the simple π exchange $g_{PS}(\pi)(f_\pi^2/4\pi=0.081)$ is given. As was already stated, it results in being close to the full g_{PS}.

Equation (20) sums all cluster diagrams factorizable in products of *dressed* two-body diagrams. Nonfactorizable diagrams involving three particles have also been taken into account, even if they do not appear in the expression.

Operatorial correlations were introduced in Ref. [23] for the spin responses within both the dressed two-body (D2B) and the SOC approximations. In the first approximation cluster diagrams containing Jastrow correlations are summed to all orders, while contributions from the other components are evaluated at the two-body level (it corresponds to the W_0 approximation of Ref. [20]). The D2B approximation came out to be very accurate and it has been used here to evaluate the IA response. A linearized version of this approximation (D2B/L), including only contributions linear in $f^{\sigma\tau,t\tau}$, has been adopted for the MEC matrix elements. However, in some cases quadratic terms, as well as those containing the other operatorial components, have been computed and checked to give small corrections.

Following the above scheme for the treatment of the $q>1$ correlations, $\xi_{PS,C}$ has an exchange part $\xi^{\rm exch}_{PS,C}$ obtained by the replacements

$$g_{cc}(r)\hat{\mathbf{r}}\rightarrow g_{cc}(r)\hat{\mathbf{r}}\left\{1+2\frac{f^{\sigma\tau}(r)-4f^{t\tau}(r)}{f^J(r)}\right\}, \tag{21}$$

$$g_{cc}(r)\imath(\sigma\times\hat{\mathbf{r}})\rightarrow g_{cc}(r)\imath(\sigma\times\hat{\mathbf{r}})\left\{1+2\frac{f^{\sigma\tau}(r)-f^{t\tau}(r)}{f^J(r)}\right\}, \tag{22}$$

in Eq. (20), and a direct one

$$\xi^{\rm dir}_{PS,C}(\mathbf{q};\mathbf{p},\mathbf{h})=\delta_{\mathbf{q}-\mathbf{p}+\mathbf{h}}\imath C_{PS}\frac{6\tau_z}{\sqrt{D(p)D(h)}}\rho_0\int d\mathbf{r}g_{PS}(r)\times[g_{dd}(r)+g_{de}(r)]e^{\imath\mathbf{q}\cdot\mathbf{r}}2\imath(\sigma\times\hat{\mathbf{r}})\times\left\{\frac{f^{\sigma\tau}(r)-f^{t\tau}(r)}{f^J(r)}\right\}, \tag{23}$$

where $g_{dd,de}(r)$ are the direct-direct and direct-exchange FHNC partial distribution functions.

$\mathbf{j}^{(2)}_{PS,C}(\mathbf{q})$ is the leading two-body current and it is the only one used to estimate $R_T^{\rm MEC}(q,\omega)$ of Eq. (14).

$\mathbf{j}^{(2)}_{PS,\pi}(\mathbf{q})$ is the sum of several components. Following an obvious notation, we will refer to the corresponding parts of its matrix element as $\xi_{PS,\pi}(G_{PS,\alpha=1,7})$. They are given in the Appendix.

In presenting the matrix elements of the $\mathbf{j}^{(2)}_{\rm MD}(\mathbf{q})$ current, $\xi_{\rm MD}(\mathbf{q};\mathbf{p},\mathbf{h})=\langle 0|\mathbf{j}^{(2)}_{\rm MD}(\mathbf{q})|\mathbf{p},\mathbf{h}\rangle$, we introduce, for the sake of brevity, the notation

$$C_\Delta=\tfrac{2}{9}G_\Delta(q,\omega)\mu_{\gamma N\Delta};f_1^\Delta(r)=u_{PT}^{\sigma\tau\rm II}(r)-u_{PT}^{t\tau\rm II}(r);f_2^\Delta(r)=3u_{PT}^{\sigma\tau\rm II}(r). \tag{24}$$

$\xi_{\rm MD}$ is given by

$$\xi_{\rm MD}(\mathbf{q};\mathbf{p},\mathbf{h})=\xi^{dir}_{\rm MD}(\mathbf{q};\mathbf{p},\mathbf{h})+\xi^{\rm exch}_{\rm MD}(\mathbf{q};\mathbf{p},\mathbf{h}), \tag{25}$$

where

$$\begin{aligned}\xi^{\rm dir}_{\rm MD}(\mathbf{q};\mathbf{p},\mathbf{h})=&\,\delta_{\mathbf{q}-\mathbf{p}+\mathbf{h}l}C_\Delta q\frac{4\tau_z}{\sqrt{D(p)D(h)}}\rho_0\int d\mathbf{r}[g_{dd}(r)+g_{de}(r)]e^{i\mathbf{q}\cdot\mathbf{r}}\Bigg\{f_1^\Delta(r)\Bigg[(\sigma\times\hat{\mathbf{q}})\Bigg(1+\frac{2f^{\sigma\tau}(r)+f^{t\tau}(r)}{f^J(r)}\Bigg)\\&-3(\sigma\cdot\hat{\mathbf{r}})(\hat{\mathbf{r}}\times\hat{\mathbf{q}})\frac{f^{t\tau}(r)}{f^J(r)}\Bigg]+f_2^\Delta(r)\Bigg[(\sigma\times\hat{\mathbf{q}})\Bigg(\frac{2f^{\sigma\tau}(r)-f^{t\tau}(r)}{f^J(r)}\Bigg)+(\sigma\cdot\hat{\mathbf{r}})(\hat{\mathbf{r}}\times\hat{\mathbf{q}})\Bigg(1+\frac{f^{t\tau}(r)-f^{\sigma\tau}(r)}{f^J(r)}\Bigg)\Bigg]\Bigg\}\\&+\delta_{\mathbf{q}-\mathbf{p}+\mathbf{h}l}C_\Delta q\frac{4\tau_z}{\sqrt{D(p)D(h)}}\rho_0\int d\mathbf{r}[g_{dd}(r)+g_{de}(r)][(\sigma\times\hat{\mathbf{q}})+(\sigma\cdot\hat{\mathbf{r}})(\hat{\mathbf{r}}\times\hat{\mathbf{q}})]\\&+\Bigg\{3f_1^\Delta(r)\frac{f^{\sigma\tau}(r)}{f^J(r)}+f_2^\Delta(r)\Bigg(\frac{2f^{t\tau}(r)+f^{\sigma\tau}(r)}{f^J(r)}\Bigg)\Bigg\},\end{aligned} \tag{26}$$

$$\begin{aligned}\xi^{\rm exch}_{\rm MD}(\mathbf{q};\mathbf{p},\mathbf{h})=&\,\delta_{\mathbf{q}-\mathbf{p}+\mathbf{h}l}C_\Delta q\frac{2\tau_z}{\sqrt{D(p)D(h)}}\rho_0\int d\mathbf{r}g_{cc}(r)[e^{i\mathbf{p}\cdot\mathbf{r}}+e^{i\mathbf{h}\cdot\mathbf{r}}]\Bigg\{f_1^\Delta(r)\Bigg[(\sigma\times\hat{\mathbf{q}})\Bigg(4+3\frac{8f^{\sigma\tau}(r)-f^{t\tau}(r)}{f^J(r)}\Bigg)\\&-9(\sigma\cdot\hat{\mathbf{r}})(\hat{\mathbf{r}}\times\hat{\mathbf{q}})\frac{f^{t\tau}(r)}{f^J(r)}\Bigg]+f_2^\Delta(r)\Bigg[(\sigma\times\hat{\mathbf{q}})\Bigg(1+2\frac{f^{\sigma\tau}(r)-f^{t\tau}(r)}{f^J(r)}\Bigg)+(\sigma\cdot\hat{\mathbf{r}})(\hat{\mathbf{r}}\times\hat{\mathbf{q}})\Bigg(1+6\frac{3f^{\sigma\tau}(r)-f^{t\tau}(r)}{f^J(r)}\Bigg)\Bigg]\Bigg\}.\end{aligned} \tag{27}$$

It is worth noticing that the second integral in the right-hand side (rhs) of Eq. (26) gives a correction independent of the modulus of $\mathbf{q}$ and vanishing for uncorrelated wave functions as well as for Jastrow correlated ones.

Figure 2 compares the $f^\Delta_{1,2}$ functions obtained with the Argonne v_{28} potential $f^\Delta_{1,2}(A_{28})$ with those from the OPE potential $f^\Delta_{1,2}(\pi)$. They differ from each other at short distances, and are therefore expected to provide similar results in a correlated model.

IV. RESULTS AND DISCUSSION

In this section we present and discuss the inclusive transverse electromagnetic response of symmetric nuclear matter at saturation density, $\rho_0=0.16$ fm^{-3} or $k_F=1.33$ fm^{-1}, as obtained in CBF theory. We recall that the correlation operator contains Jastrow, spin, tensor, and isospin components. The correlations are fixed by minimizing the ground state energy, computed in FHNC SOC approximation and using the Argonne v_{14}+Urbana VII three-nucleon interaction [34]. The SPR model for the two-body current operators of Refs. [18,27] has been used and the one-body current is given by the magnetization part alone, neglecting the convection term. The response is computed including correlated $1p1h$ intermediate states and then folding $R_T^{1p1h}(q,\omega)$ with a parametrization of the on-shell imaginary part of the CBF optical potential.

We begin by studying the effect of the Jastrow, short range correlations and comparing with the free Fermi gas. The $1p1h$ responses in both models are given in Fig. 3 at $q=300$ (a), 400 (b), and 550 (c) MeV/c. In the figures the one-body response (IA), the interference terms between one-body and $\mathbf{j}^{(2)}_{PS,C}(\mathbf{q})$ (OB/C), one-body and $\mathbf{j}^{(2)}_{PS,\pi}(\mathbf{q})$ (OB/π), one-body and $\mathbf{j}^{(2)}_{\rm MD}(\mathbf{q})$ (OB/Δ), and the quadratic $\mathbf{j}^{(2)}_{PS,C}(\mathbf{q})$ (C/C) term are shown, together with the resulting total response (TOT).

The shift of the Jastrow responses to higher energies with respect to the FG is due to the use of the CBF real part of the optical potential; moreover, as in the case of the longitudinal response [10], Jastrow correlations quench the quasielastic peaks in absolute magnitude. The computed quadratic term is always negligible and will be disregarded in the remainder of the paper. Two interference responses (OB/C and OB/Δ) have been evaluated also for the one-pion-exchange currents. The results at $q=400$ MeV/c are displayed in Fig. 3(b) as up and down triangles, respectively. They are almost coincident with the SPR responses, as the differences in the short range behaviors of the Δ currents are washed out by the correlation.

The numerical accuracy of the FG responses has been checked against the analytical approach of Ref. [17] finding complete agreement. So an overall reduction of the $1p1h$ QE peak due to MEC's is confirmed in the FG model and found even in the Jastrow correlated case.

As we have already mentioned in the Introduction, this result is in sharp contrast with realistic estimates of the transverse response in light nuclei [11] and also with some recent random phase approximation (RPA) calculations in ^{12}C [35], both of them pointing to a $\sim 20-30\%$ increase of the strength in the quasielastic region due to MEC effects. We

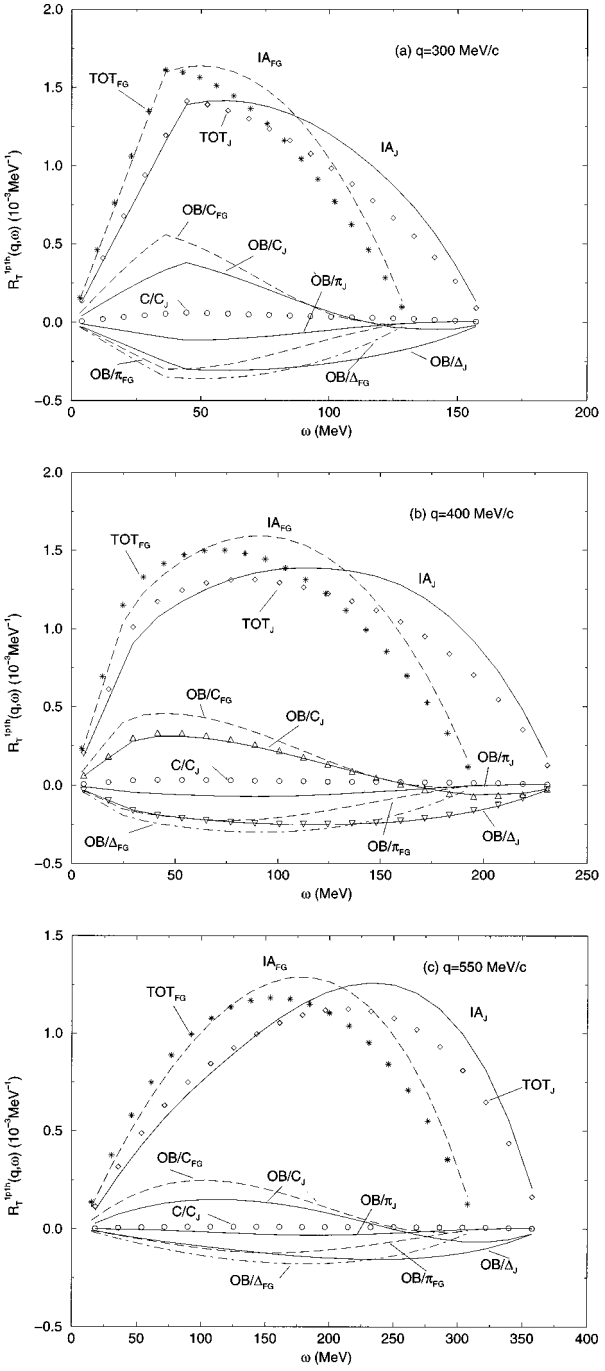

FIG. 3. $1p1h$ transverse response at $q=300$ (a), 400 (b), and 550 (c) MeV/c for the FG and Jastrow models. The figure shows the partial (one-body, interference, and one quadratic) and the total responses. The interference terms for the contact (triangles up) and Δ (triangles down) currents in the one-pion-exchange model at $q=400$ MeV/c are given.

stress once again that this conflict is not resolved by the inclusion of state-independent, scalar, short range correlations.

In Ref. [23] it was shown that the transverse spin responses, making up $R_T^{\mathrm{IA}}(q,\omega)$, may be affected by the non-Jastrow correlations. In particular, the largest effect was found in the isovector $S_{T,\sigma}^{\tau=1}$, as the leading correction is proportional to the large tensor-isospin correlation $f^{t\tau}(r)$.

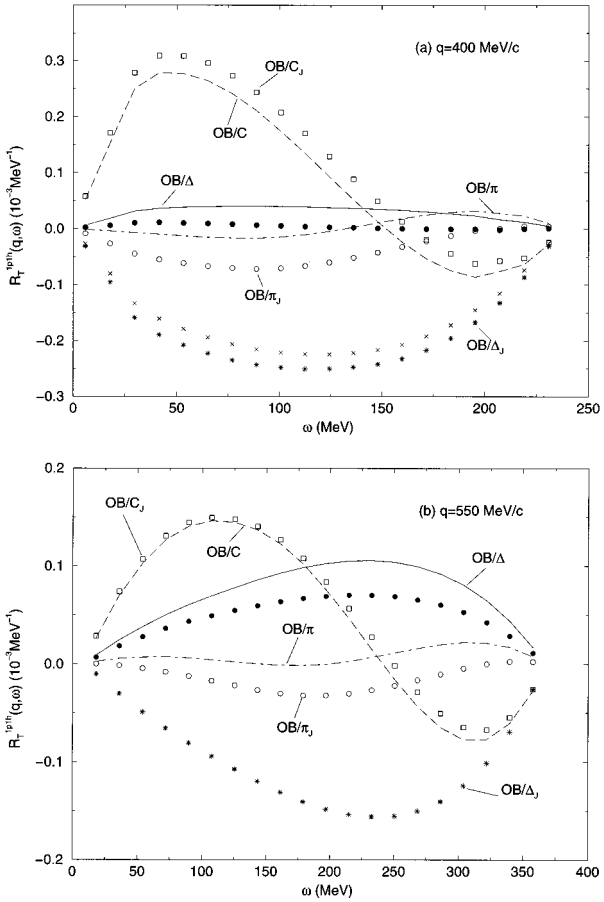

FIG. 4. $1p1h$ interference responses at $q=400$ (a) and 550 (b) MeV/c in the correlation operator model and comparison with the Jastrow model. See text.

Hence, the correlation operator (3) has been used to estimate the corrections to the Jastrow response due to the nonscalar components, in the D2B/L approximation.

Figure 4(a) reports the correlation operator results for the interference $1p1h$ responses at $q=400$ MeV/c. We find that, at the QE peak, the operatorial correlations quench the OB/C and OB/π responses with respect to the Jastrow case. The use of the D2B in place of the D2B/L approximation does not change appreciably the outcome. The quenching is more pronounced for the OB/π term, where a positive tail is added at large energies.

The effect is dramatic in OB/Δ, as the correlation operator correction largely cancels the Jastrow response, yielding a positive net result. The origin of this cancellation is found in the tensor-isospin correlation contribution to the second integral in the RHS of Eq. (26). In fact, the OB/Δ response obtained by setting $f^{t\tau}=0$ in the integral is much closer to the Jastrow curve, as is shown in the figure by the $\times$ signs. The convergence of the cluster expansion has been checked by computing the integral (i) in D2B approximation and (ii) adding Jastrow dressed three-body nonfactorizable diagrams, linear in the operatorial components of the correlation. The result is practically indistinguishable from the D2B/L response and it is not given in the figure.

A similar (and even more enhanced) behavior is found at

larger momenta. In Fig. 4(b) we show the interference terms at $q=550$ MeV/c. Now the OB/C response does not significantly differ from the Jastrow estimate, whereas OB/π and OB/Δ are largely modified by the insertion of the operatorial correlations. In particular, we obtain a large, positive OB/Δ component in place of a large, negative Jastrow counterpart. At this momentum transfer and using only long range RPA correlations, the Gent group seems to find a more negative OB/π response and an almost vanishing OB/Δ one [36].

The sensitivity of the OB/Δ response to the shape of $f^{t\tau}$ has been examined by using the correlation operator corresponding to the Urbana v_{14}+TNI model. This interaction has a weaker tensor component, producing a smaller tensor correlation. The results for OB/Δ are displayed in Fig. 4 as solid circles and point to a clear dependence on the details of this correlation.

To conclude the analysis of the $1p1h$ response, we give in Fig. 5 the total $R_T^{1p1h}(q,\omega)$ together with the IA estimate. The total (TOT) response includes interference contributions also from the $\mathbf{j}_V^{(2)}(\mathbf{q})$ and $\mathbf{j}_{VS}^{(2)}(\mathbf{q})$ currents, whereas the curves labeled as TOT_{PS} only contain $\mathbf{j}_{PS}^{(2)}(\mathbf{q})$ (as the Jastrow, TOT_J, points). MEC's provide an enhancement of the IA response in the QE region ranging from $\sim$20% at $q=300$ MeV/c to $\sim$10% at $q=550$ MeV/c. The enhancement is due to the presence of tensor- and isospin-dependent correlations; scalar Jastrow correlations actually produce MEC contributions, quenching the corresponding IA values. The exchange of ρ-like vector mesons, originating the V and VS currents, results in an additional enhancement of $R_T^{1p1h}(q,\omega)$, which, however, decreases with q.

Finally, we compare the transverse NM response with some of the available experimental data from real life nuclei. $R_T(q,\omega)$ is obtained by folding the computed $R_T^{1p1h}(q,\omega)$ with the imaginary part of the optical potential, as described in Sec. II. Figures 6 compare $A\times R_T(q,\omega)$ of NM in IA and IA+MEC with data from Ref. [4] ($\times$), Ref. [6] (circles), and Ref. [9] (black circles) for ^{40}Ca. The Bates data [6] actually refer to $q=330$ MeV/c in Fig. 6(a) and $q=400$ MeV/c in Fig. 6(b), as the Saclay data (Ref. [4]) in the same figure. The discrepancies between the Saclay and the Bates and Jourdan [9] results are evident and already stressed in previous literature. It must be noticed that the last two sets of data appear to be compatible among each other. This fact gives confidence in the Jourdan's L/T separation procedure, which employs world data on inclusive quasielastic electron scattering as obtained by different experiments.

The NM responses are closer to the results of Refs. [6,9] than to those of Ref. [4] and the experimental QE peak lies between the IA and the full responses. At $q=300$ MeV/c the IA seems to better reproduce the peak, whereas, when moving to higher momenta, the inclusion of MEC's improves the agreement with the experiments.

A similar trend is found in ^{56}Fe, as shown in Fig. 7.

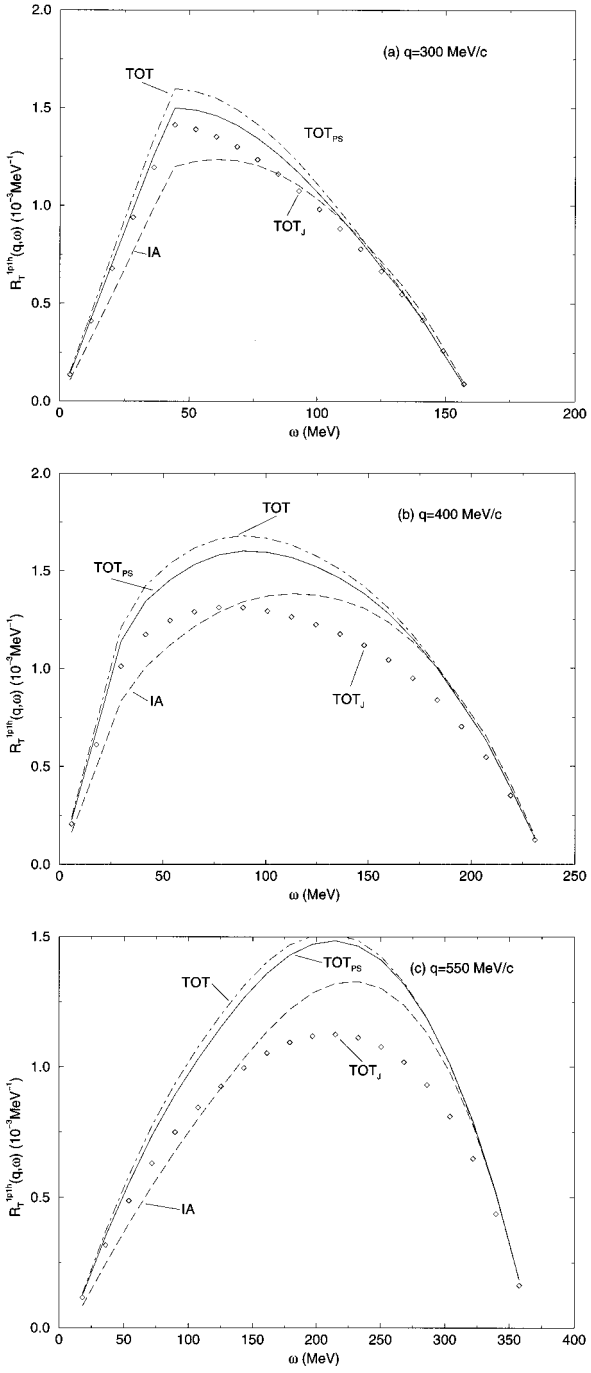

FIG. 5. Total $1p1h$ responses at $q=300$ (a), 400 (b), and 550 (c) MeV/c in the correlation operator model and comparison with the Jastrow model and the IA responses. See text.

V. CONCLUSIONS

The inclusive electromagnetic transverse response of symmetric nuclear matter has been evaluated within the correlated basis function perturbation theory. The adopted correlation operator has a scalar, short range component and important tensor- and isospin-dependent parts, its structure being similar to that of realistic nucleon-nucleon potentials. Both one-body and two-body meson exchange currents are considered, the latter in a model which satisfies the continuity equation with the Argonne v_{14} potential and contains in-

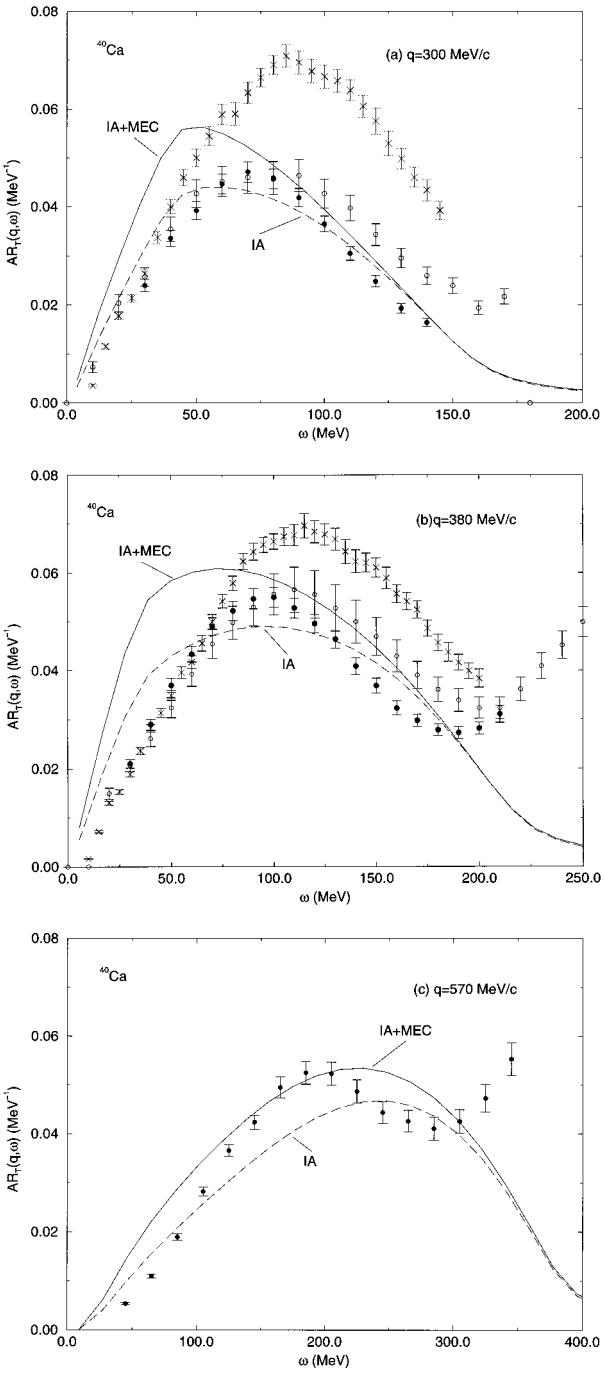

FIG. 6. Transverse responses at $q=300$ (a), 380 (b), and 570 (c) MeV/c for ^{40}Ca and nuclear matter. See text.

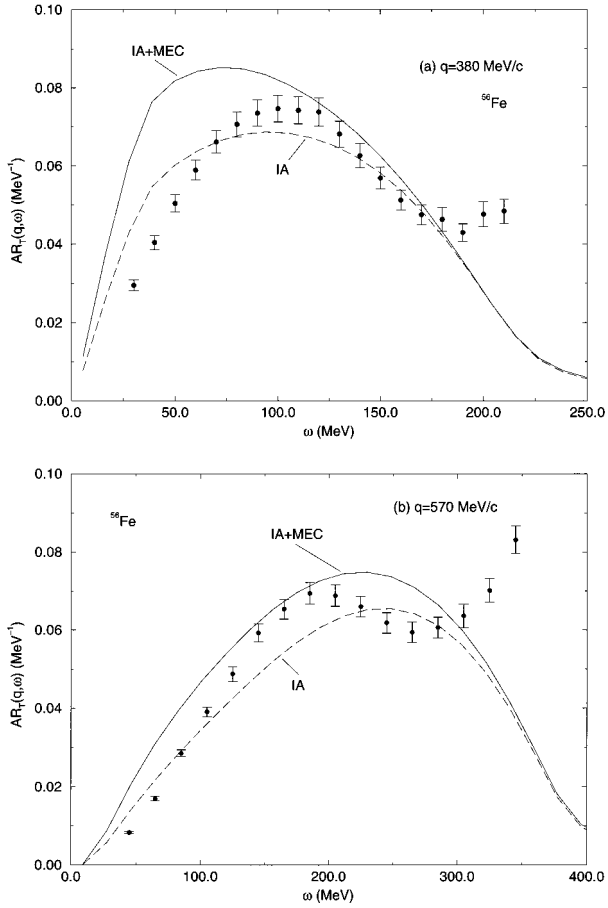

FIG. 7. Transverse responses at $q=380$ (a) and 570 (b) MeV/c for ^{56}Fe and nuclear matter. See text.

termediate Δ-isobar excitation currents. Ground and $1p1h$ correlated states are included and the decay into $2p2h$ states is implemented by folding $R_T^{1p1h}(q,\omega)$ with the imaginary part of the optical potential.

Our results indicate that MEC's, evaluated in a Jastrow correlated model, quench the IA response. In this case, the situation is qualitatively close to what was found by Amaro *et al.* in Ref. [17] in both shell and Fermi gas models. The net quenching mainly originates from a strong cancellation between the positive contact and the negative Δ terms.

The introduction of tensor-isospin-dependent correlations drastically changes this picture. The Δ contribution is largely modified, as it becomes positive and increasing with the momentum transfer. As a result, MEC's produce an extra strength (10–20 %) in the QE peak region. This is in agreement with exact GFMC calculations in light nuclei.

ρ-like exchange currents give a small additional enhancement. We also found that using standard one-boson-exchange currents does not significantly change our results.

Two recently derived experimental responses in ^{40}Ca have consistently lowered the QE peak respect to previous estimates. The new data and the CBF NM responses are in reasonable agreement and the comparison seems to show too large MEC effects at low momenta. The obvious caveat to bear in mind is that this comparison is made between finite nuclear systems and infinite, homogenous nuclear matter. The CBF theory has been recently extended [37] to deal with ground state properties of nuclei as heavy as ^{208}Pb, with Jastrow and isospin-dependent correlations. It is conceivable that, in the near future, it will be possible to use the theory to microscopically compute the finite nuclei responses, employing richer correlations, as those of nuclear matter. Presently, the density-dependent NM results might be used in a local density approximation for a closer comparison with the experiments.

Moreover, relativistic corrections could affect the

response, both for the IA and MEC's [38], as well as the inclusion of explicit Δ degrees of freedom in the nuclear wave function. This last topic may be addressed within CBF theory, particularly if one wants to quantitatively study the dip and Δ peak regions. In this respect, it will also be necessary to consider the contribution from $2p2h$ intermediate correlated states. Work along these lines is in progress.

ACKNOWLEDGMENTS

The author wants to thank Rocco Schiavilla for many fruitful discussions and Juerg Jourdan for providing his data on Ca and Fe. The warm hospitality of TJNAF (ex CEBAF) laboratory, where part of this work has been done, is also gratefully acknowledged.

APPENDIX

In this appendix the particle-hole nondiagonal matrix elements of the components of $\mathbf{j}^{(2)}_{PS,\pi}(\mathbf{q})$ are given in the D2B/L approximation:

$$\xi^{\rm dir}_{PS,\pi}(G_{PS,1}) = \delta_{\mathbf{q}-\mathbf{p}+\mathbf{h}\,\imath} C_{PS} \frac{6\tau_z}{\sqrt{D(p)D(h)}} \rho_0 \int d\mathbf{r} \frac{G_{PS,1}(\mathbf{r})}{r^2} [g_{dd}(r)+g_{de}(r)] e^{\imath \mathbf{q}\cdot\mathbf{r}/2} \left[6\imath(\sigma\times\hat{\mathbf{r}}) \frac{f^{t\tau}(r)}{f^J(r)} \right], \tag{A1}$$

$$\xi^{\rm exch}_{PS,\pi}(G_{PS,1}) = \delta_{\mathbf{q}-\mathbf{p}+\mathbf{h}\,\imath} C_{PS} \frac{6\tau_z}{\sqrt{D(p)D(h)}} \rho_0 \int d\mathbf{r} \frac{G_{PS,1}(\mathbf{r})}{r^2} g_{cc}(r) e^{\imath \mathbf{Q}\cdot\mathbf{r}} \left[2\hat{\mathbf{r}} \left(\frac{5f^{\sigma\tau}(r) - 8f^{t\tau}(r)}{f^J(r)} \right) - \imath(\sigma\times\hat{\mathbf{r}}) \frac{f^{t\tau}(r)}{f^J(r)} \right], \tag{A2}$$

$$\xi^{\rm dir}_{PS,\pi}(G_{PS,2+3}) = \delta_{\mathbf{q}-\mathbf{p}+\mathbf{h}\,\imath} C_{PS} \frac{6\tau_z}{\sqrt{D(p)D(h)}} \rho_0 \int d\mathbf{r} \left[\frac{G_{PS,2}(\mathbf{r}) + G_{PS,3}(\mathbf{r})}{r} \right] [g_{dd}(r)+g_{de}(r)]$$
$$\times e^{\imath \mathbf{q}\cdot\mathbf{r}/2} \left[[3(\mathbf{q}\cdot\hat{\mathbf{r}})(\sigma\times\hat{\mathbf{r}}) - 3\hat{\mathbf{r}}(\sigma\times\hat{\mathbf{r}})\cdot\mathbf{q} - 2(\sigma\times\mathbf{q})] \frac{f^{t\tau}(r)}{f^J(r)} - 2(\sigma\times\mathbf{q}) \frac{f^{\sigma\tau}(r)}{f^J(r)} \right], \tag{A3}$$

$$\xi^{\rm exch}_{PS,\pi}(G_{PS,2+3}) = \delta_{\mathbf{q}-\mathbf{p}+\mathbf{h}\,\imath} C_{PS} \frac{6\tau_z}{\sqrt{D(p)D(h)}} \rho_0 \int d\mathbf{r} \left[\frac{G_{PS,2}(\mathbf{r}) + G_{PS,3}(\mathbf{r})}{r} \right] g_{cc}(r)$$
$$\times e^{\imath \mathbf{Q}\cdot\mathbf{r}} \left[(\sigma\times\mathbf{q}) - 3[(\mathbf{q}\cdot\hat{\mathbf{r}})(\sigma\times\hat{\mathbf{r}}) + (\sigma\cdot\hat{\mathbf{r}})(\mathbf{q}\times\hat{\mathbf{r}})] \frac{f^{t\tau}(r)}{f^J(r)} \right], \tag{A4}$$

$$\xi^{\rm dir}_{PS,\pi}(G_{PS,4+5}) = \delta_{\mathbf{q}-\mathbf{p}+\mathbf{h}\,\imath} C_{PS} \frac{6\tau_z}{\sqrt{D(p)D(h)}} \rho_0 \int d\mathbf{r} \left[\frac{G_{PS,4}(\mathbf{r}) + G_{PS,5}(\mathbf{r})}{r} \right] [g_{dd}(r)+g_{de}(r)]$$
$$\times e^{\imath \mathbf{q}\cdot\mathbf{r}/2} \left[\hat{\mathbf{r}}(\sigma\times\hat{\mathbf{r}})\cdot\mathbf{q} \left(\frac{f^{t\tau}(r) - 2f^{\sigma\tau}(r)}{f^J(r)} \right) \right], \tag{A5}$$

$$\xi^{\rm exch}_{PS,\pi}(G_{PS,4+5}) = -\delta_{\mathbf{q}-\mathbf{p}+\mathbf{h}\,\imath} C_{PS} \frac{6\tau_z}{\sqrt{D(p)D(h)}} \rho_0 \int d\mathbf{r} \left[\frac{G_{PS,4}(\mathbf{r}) + G_{PS,5}(\mathbf{r})}{r} \right] g_{cc}(r) e^{\imath \mathbf{Q}\cdot\mathbf{r}} [\hat{\mathbf{r}}(\sigma\times\hat{\mathbf{r}})\cdot\mathbf{q}], \tag{A6}$$

$$\xi^{\rm dir}_{PS,\pi}(G_{PS,6}) = 0, \tag{A7}$$

$$\xi^{\rm exch}_{PS,\pi}(G_{PS,6}) = -\delta_{\mathbf{q}-\mathbf{p}+\mathbf{h}\,\imath} C_{PS} \frac{6\tau_z}{\sqrt{D(p)D(h)}} \rho_0 \int d\mathbf{r} G_{PS,6}(\mathbf{r}) g_{cc}(r) e^{\imath \mathbf{Q}\cdot\mathbf{r}} \left[3\imath\hat{\mathbf{r}}(\mathbf{q}\cdot\hat{\mathbf{r}})(\sigma\times\hat{\mathbf{r}})\cdot\mathbf{q} \frac{f^{t\tau}(r)}{f^J(r)} \right], \tag{A8}$$

$$\xi^{\rm dir}_{PS,\pi}(G_{PS,7}) = \xi^{\rm exch}_{PS,\pi}(G_{PS,7}) = 0, \tag{A9}$$

where $\mathbf{Q} = (\mathbf{p}+\mathbf{h})/2$.

[1] E.J. Moniz *et al.*, Phys. Rev. Lett. **26**, 445 (1971).
[2] P. Barreau *et al.*, Nucl. Phys. **A402**, 515 (1981).
[3] M. Deady *et al.*, Phys. Rev. C **28**, 631 (1983).
[4] Z. Meziani *et al.*, Phys. Rev. Lett. **52**, 2130 (1984).
[5] R. Altemus *et al.*, Phys. Rev. Lett. **44**, 965 (1980).
[6] T.C. Yates *et al.*, Phys. Lett. B **312**, 382 (1993).
[7] A. Zghiche *et al.*, Nucl. Phys. **A572**, 513 (1994).
[8] J. Jourdan, Phys. Lett. B **353**, 189 (1995).

[9] J. Jourdan, Nucl. Phys. **A603**, 117 (1996).
[10] A. Fabrocini and S. Fantoni, Nucl. Phys. **A503**, 375 (1989).
[11] J. Carlson, Few-Body Syst. Suppl. **8**, 32 (1995).
[12] R.B. Wiringa, R.A. Smith, and T.L. Ainsworth, Phys. Rev. C **29**, 1207 (1984).
[13] A. De Pace and M. Viviani, Phys. Rev. C **48**, 2931 (1993).
[14] W. Alberico, R. Cenni, and A. Molinari, Prog. Part. Nucl. Phys. **23**, 171 (1989).
[15] J.W. Van Orden and T.W. Donnelly, Ann. Phys. (N.Y.) **131**, 451 (1981).
[16] W. Alberico, M. Ericson, and A. Molinari, Ann. Phys. (N.Y.) **154**, 356 (1984).
[17] J.E. Amaro, G. Co', and A.M. Lallena, Nucl. Phys. **A578**, 365 (1994).
[18] R. Schiavilla, V.R. Pandharipande, and D.O. Riska, Phys. Rev. C **40**, 2294 (1989).
[19] S. Rosati, in *From Nuclei to Particles*, Proceedings of the International School of Physics E. Fermi, Varenna, edited by A. Molinari (North-Holland, Amsterdam, 1981), p. 73.
[20] V.R. Pandharipande and R.B. Wiringa, Rev. Mod. Phys. **51**, 821 (1979).
[21] R.B. Wiringa, V. Fiks, and A. Fabrocini, Phys. Rev. C **38**, 1010 (1988).
[22] I.E. Lagaris and V.R. Pandharipande, Nucl. Phys. **A359**, 331 (1981);**A359**, 349 (1981).
[23] A. Fabrocini, Phys. Lett. B **322**, 171 (1994); in *Condensed Matter Theories*, edited by M. Casas, M. De Llano, and A. Polls (Nova Science, New York, 1995), Vol. X, p. 147.
[24] S. Fantoni and V.R. Pandharipande, Nucl. Phys. **A473**, 234 (1987).
[25] R. Schiavilla, Nucl. Phys. **A499**, 301 (1989).
[26] D.O. Riska, *Mesons in Nuclei*, edited by M. Rho and D. Wilkinson (North-Holland, Amsterdam, 1979), Vol. II, p. 755; Prog. Part. Nucl. Phys. **11**, 199 (1984).
[27] R. Schiavilla, R.B. Wiringa, V.R. Pandharipande, and J. Carlson, Phys. Rev. C **45**, 2628 (1992).
[28] R. Schiavilla (private communication).
[29] G.E. Brown and W. Weise, Phys. Rep. **22**, 279 (1975).
[30] A. Fabrocini and S. Fantoni, Phys. Lett. B **298**, 263 (1993).
[31] S. Fantoni and V.R. Pandharipande, Nucl. Phys. **A427**, 473 (1984).
[32] O. Benhar, A. Fabrocini, and S. Fantoni, Nucl. Phys. **A505**, 267 (1989).
[33] O. Benhar *et al.*, Phys. Rev. C **44**, 2328 (1991).
[34] R. Schiavilla, V.R. Pandharipande, and R.B. Wiringa, Nucl. Phys. **A449**, 219 (1986).
[35] V. Van der Sluys, J. Ryckebusch, and M. Waroquier, Phys. Rev. C **51**, 2664 (1995).
[36] V. Van der Sluys (private communication).
[37] F. Arias de Saavedra, G. Co, A. Fabrocini, and S. Fantoni, Nucl. Phys. **A605**, 359 (1996).
[38] P.G. Blunden and M.N. Butler, Phys. Lett. B **219**, 151 (1989).